ELSEVIER

International Journal of Mass Spectrometry 195/196 (2000) 653–666

International Journal of Mass Spectrometry

A vibrationally resolved negative ion photoelectron spectrum of Nb_8

Timothy P. Marcy[1], Doreen G. Leopold*

Department of Chemistry, University of Minnesota, Minneapolis, MN 55455, USA

Received 12 August 1999; accepted 24 August 1999

Abstract

The 488 nm negative ion photoelectron spectrum of Nb_8, obtained at an instrumental resolution of ~5 meV, displays a clear vibrational progression in a mode with a frequency of 180 ± 15 cm^{-1} in neutral Nb_8 and 165 ± 20 cm^{-1} in Nb_8^-. The normal mode displacement of 0.4 ± 0.1 $u^{1/2}$ Å indicates a very small geometry change upon electron detachment. The electron affinity of Nb_8 is 1.513 ± 0.008 eV. These results are discussed in light of previous negative ion photoelectron spectroscopic and density functional studies of Nb_8 and Nb_8^-. (Int J Mass Spectrom 195/196 (2000) 653–666) © 2000 Elsevier Science B.V.

Keywords: Niobium clusters; Metal clusters; Metal ions; Photoelectron spectroscopy

1. Introduction

Our understanding of bare and partially ligated transition metal clusters has made enormous progress during the past decade [1–10]. A battery of spectroscopic techniques [1–3,6,7,9,10], including resonant two-photon ionization, laser-induced fluorescence, resonance Raman, electron spin resonance, and photoelectron [11–13] spectroscopies, has yielded a wealth of data concerning the electronic structures and bonding of these complex systems. For the smallest clusters containing just three metal atoms, a broad database of vibrational frequency measurements is also available [10,14–29]. Vibrationally resolved spectra have been reported for the homonuclear trimers of Sc [14], Zr [15], Hf [15], V [16], Nb [17], Cr [18], Mn [19], Ni [20], Pd [21], Pt [21], Cu [22], Ag [23], and Au [24], several mixed coinage metal trimers [25], and the metal-ligand clusters Nb_3O [26], Nb_3N_2 [27], Nb_3C_2 [28], Y_3C_2 [29] and their cations. In contrast, there are only rare examples of transition metal clusters with more than three metal atoms that have been vibrationally characterized in mass selected experiments. These include the early transition metal tetramer Ta_4 [30], and several coinage metal clusters (e.g. Cu_4^+ [31], Ag_5 [32], Au_4 [33], Au_6 [33,34], and Au_6^- [34]). Data of this type, when combined with theoretical studies that are increasingly able to accurately predict vibrational frequencies for metal clusters and partially ligated complexes [5], would help to identify the structures of these larger clusters while also providing benchmarks for evaluating computational methods.

* Corresponding author. E-mail: dleopold@chem.umn.edu

[1] Present address: Joint Institute for Laboratory Astrophysics; University of Colorado, Boulder, CO 80309-0440.

Dedicated to the memory of Professor Bob Squires.

PII S1387-3806(99)00182-7

We report here a vibrationally resolved negative ion photoelectron spectrum of Nb_8. For the monovalent alkali and coinage metals, eight-atom clusters have shown exceptional stabilities, which have been successfully interpreted using electronic shell models [3,35]. Although Nb_8 is an early transition metal cluster of pentavalent atoms (Nb has a $^6D\ (4d)^4(5s)^1$ ground state) [36], it too exhibits an anomalous stability in several respects. Flow tube studies have shown that the reactivity of neutral Nb_8 with D_2 and N_2 is dramatically lower than that of niobium clusters of similar size, with the exception of Nb_{10} and Nb_{16}, which are also relatively unreactive [37–40]. Studies of positively [41–43] and negatively [42] charged niobium cluster ions have yielded analogous results. Since a critical step in the dissociative chemisorption of D_2 and N_2 is thought to involve charge transfer from the metal to weaken the diatomic bond, the increased ionization potentials measured [44–46] for Nb_8, Nb_{10}, and Nb_{16} have led some to conclude that this property largely explains their low reactivities [40,44]. Others have emphasized the independence of the reactivity pattern on the charge state of the cluster and have concluded that its geometrical structure must play an important role [8,43].

Nb_8 provides a particularly challenging subject for theorists, due to its open *d*-shell atomic configuration and the plethora of possible structural isomers. There are 257 nonisomorphic convex polyhedra with eight vertices, which have been completely catalogued by Britton and Dunitz [47]. Nevertheless, this cluster has recently been studied using density functional theory (DFT) by two groups [48–52]. Fournier and co-workers [51,52] employed the local spin density approximation (LSDA) and predicted the Nb_8^- anion to have a doublet ground state with a C_{2v} bicapped distorted octahedral structure. Three additional isomers, with C_1, D_{3d} and C_{2v} symmetries, were calculated to lie 1.05–1.64 eV above the ground state. Singlet states of neutral Nb_8, as well as doublet states of Nb_8^- and Nb_8^+, were calculated by Grönbeck et al. using the LSDA and BLYP (Becke's exchange functional with the correlation functional of Lee, Yang, and Parr) methods [50]. All three charge states were found to have the same C_{2v} ground state structure that was predicted in the earlier [51,52] study [50]. Four isomers were found to lie within 1 eV of the ground state, including the C_1 structure also identified by Fournier and co-workers [51,52], and additional D_{3d}, D_{2d}, and C_{2v} structures [50]. For Nb_8, four of the five structures (all but the D_{2d}) were predicted to have very similar electron affinities and energy spacings between the highest occupied and lowest unoccupied molecular orbitals (HOMO-LUMO gaps), as well as nonbonding LUMOs [50]. The apparent insensitivity of these electronic properties to the detailed molecular geometry emphasizes the need for vibrational and other data that may provide a more structure-sensitive probe.

Ultraviolet photoelectron spectra of the niobium cluster anions Nb_3^-–Nb_{20}^- have been reported by Kietzmann et al. [52,53]. They measured a vertical electron detachment energy of slightly under 1.5 eV for Nb_8^- (and Nb_{10}^-), 0.2 eV lower than the values measured for Nb_7^-, Nb_9^-, and Nb_{11}^- [53]. This even-odd alternation, which was reported for clusters up to Nb_{17} [53], is analogous to those observed for the alkali [54] and coinage metal [55] clusters. As for these monovalent metals, the opposite oscillation (even $>$ odd) is observed in the niobium cluster ionization potentials [44–46]. These patterns are signatures of nondegenerate frontier orbitals with singlet and doublet ground states, respectively, for neutral and ionic clusters containing even numbers of metal atoms, with the opposite assignments for the odd numbered clusters, in agreement with the DFT [48–52] results. The first excited state of Nb_8 reported in the photoelectron study lies 0.7 eV above the ground state, providing a measure of its HOMO-LUMO gap [52,53]. Relatively large gaps were measured for Nb_8, Nb_{10}, and Nb_{16} as compared with the other even clusters, a result interpreted as evidence for the dominance of electronic structure in determining the low reactivities of these three clusters with hydrogen [53]. As in previous studies of niobium clusters [39,42,43,45,56], structural isomers were in evidence. The Nb_8^- state observed in the 3.49 eV spectrum was assigned as the calculated C_{2v} doublet ground state, and changes in peak shapes with anion source condi-

tions were attributed to the additional presence of the C_1 isomer [52].

In other experimental studies, bond energies were measured by Armentrout and co-workers for Nb_2^+–Nb_{20}^+ cations dissociating to form $M_{x-1}^+ + M$ products [57]. Values of 592 kJ/mol for Nb_8^+ and (when combined with ionization potential measurements [45]) of 610 kJ/mol for Nb_8 were obtained [57]. Photodissociation studies of van der Waals complexes of Nb_n clusters ($n = 5$–20) yielded size-selective spectra with structureless absorptions increasing toward the ultraviolet [58,59].

The higher resolution photoelectron spectrum of Nb_8^- reported here provides new vibrational data. These results can potentially help to identify the observed cluster structure, and also provide a sensitive test of theoretical predictions for this computationally challenging early transition metal octamer.

2. Experimental methods

The negative ion photoelectron spectrometer used in our laboratory [60] employs a flowing afterglow ion-molecule reactor [61]. A dc cathode discharge source produces metal clusters [62], which are cooled by 10^4–10^5 collisions with the He and Ar buffer gasses and other species in the flow tube. The sampled anions are focussed and accelerated to ~1200 V by a series of electrostatic lenses, and mass selected by a 90° sector electromagnet. The mass selected anions are then decelerated to 20 V, and focussed at the intersection of the anion beam with the focussed beam of an argon ion laser. The laser is operated as a four-mirror folded cavity resonator that encloses the spectroscopy chamber to provide a circulating power of ~100 W (at 488 nm) at the laser-ion crossing. The laser is tilted at the "magic angle" [63] to produce a polarization yielding signal intensities proportional to average photodetachment cross sections. A small (3 °) solid angle of the photodetached electrons is energy-analyzed by a 6-in. radius electrostatic hemispherical analyzer operated at a pass energy of 1.5 eV, yielding a resolution of ~5 meV, and detected by a position sensitive array detector. Mass spectra are generated by scanning the electromagnet while detecting the anions at a Faraday cup that terminates the anion beam line in the spectroscopy chamber.

In the present study, cluster anions were prepared from a niobium cathode (ESPI, Ashland, OR, 99.9%) positioned 40 in. from the 2-mm-diameter nosecone sampling aperture. The cathode was held at ~−3 kV with respect to the grounded, 2-in.-diameter flow tube. With a flow rate of 6.5 SLPM (standard liters per minute) He and 0.6 SLPM Ar, a Roots pump with an effective pumping speed of 220 L/s maintained a flow tube pressure of 0.5 Torr and a bulk flow velocity of about 100 m/s. Ar^+ and other cations bombard the cathode creating niobium atoms and clusters, which can form anions (and undetected cations) through further interactions with the plasma, and grow to larger clusters by ion-neutral reactions during their ~10 ms residence time in the flow tube. Impurities in the buffer gasses were reduced by passing the He (industrial grade) through a coiled column of liquid nitrogen cooled molecular sieves and the Ar (ultra-high purity zero grade) through an oxygen-removing inert gas purifier (Oxyclear). The absolute electron kinetic energy scale was calibrated against the electron affinity of atomic oxygen [64]. The energy scale compression factor (γ), which typically has a small value of ≤0.3% in our instrument, was checked against the atomic splittings [36] in the Nb^- spectrum.

3. Results

3.1. Mass spectrum

Fig. 1 shows a mass spectrum of the anions produced by the niobium cathode discharge source, with the last 30 in. of the flow tube cooled with liquid nitrogen to enhance cluster formation. Niobium has one naturally occurring isotope (^{93}Nb). The spectrum is dominated by bare Nb_n^- clusters maximizing at Nb_4^- and Nb_5^- (~40 pA), with 2 pA (1×10^7 ions/s) of Nb_8^-. Niobium cluster monoxide anions, Nb_nO^- ($n = 4$–9), are the dominant "impurities" for the larger clusters, whereas for the smaller clusters car-

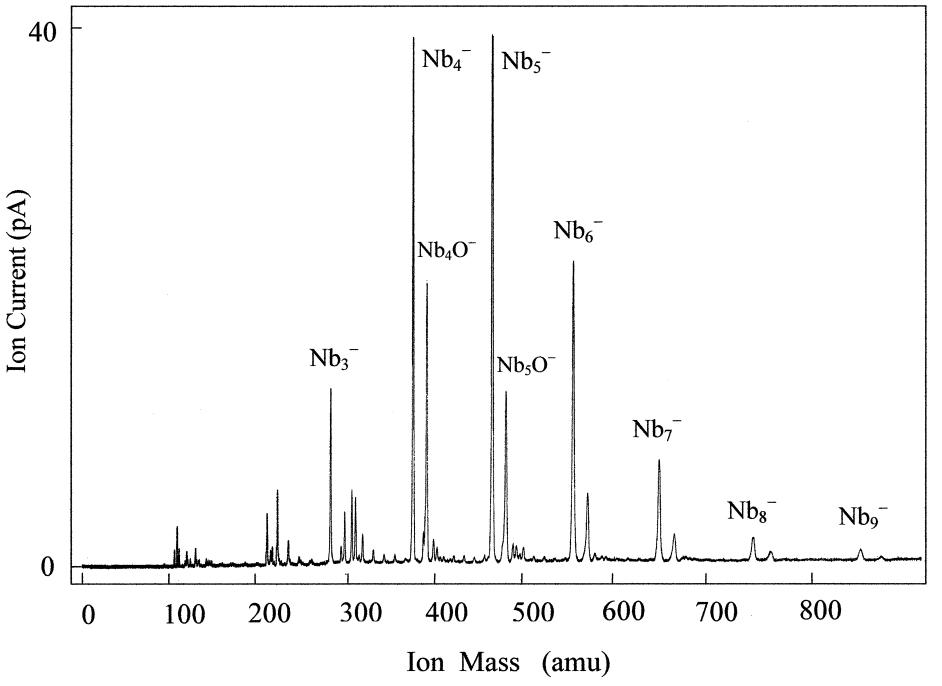

Fig. 1. Mass spectrum of anions produced by the niobium cathode discharge source in the fully cooled flow tube. Unlabelled peaks are mainly niobium carbides and oxides.

bides as well as oxides are prevalent. For example, the main anions detected containing two Nb atoms are $Nb_2C_n^-$, $n = 2$–4. The spectrum is similar to the one reported in the previous flowing afterglow study of niobium cluster anions by Mwakapumba and Ervin [65]. Although we detected no Nb^- or Nb_2^- under these conditions, the addition of even trace amounts (e.g. 0.3 cm^3/min) of benzene to the flow tube produced several picoamps of these anions [66], presumably due to fragmentation from larger reaction products [65,67]. To obtain the photoelectron spectra reported here, the mass analyzer was set to pass only Nb_8^- anions into the spectroscopy chamber. The photoelectron spectra of the other Nb_n^- ($n = 1$–9) anions have also been studied and will be reported elsewhere [68].

3.2. Photoelectron spectrum

Fig. 2 displays the photoelectron spectrum of mass-selected Nb_8^- recorded using the 488.0 nm line of the argon ion laser, and plotted as a function of the electron kinetic energy (eKE, bottom axis) and of the electron binding energy (top axis), where the latter is defined simply as the photon energy (2.540 eV) minus the measured eKE. No photoelectrons were observed above the noise level in the higher eKE region not shown in the figure. The photoelectron spectrum does not closely resemble those we obtained for any of the smaller Nb_{1-7}^- anions [68], consistent with its assignment to Nb_8^- rather than to a possible fragment anion produced from the mass-selected anion beam in a two-photon process.

The structured region of the spectrum, expanded in Fig. 3, displays a clear vibrational progression in a mode with a frequency of 180 ± 15 cm^{-1} in neutral Nb_8. Transitions to vibrational levels up to $v = 3$ are observed with successively decreasing intensities. A spectrum obtained at 514 nm displayed the same peak spacings and relative intensities, consistent with a direct photodetachment process (rather than a partially resonant process as we have observed in the spectra of other transition metal anions, such as Cr_2^-

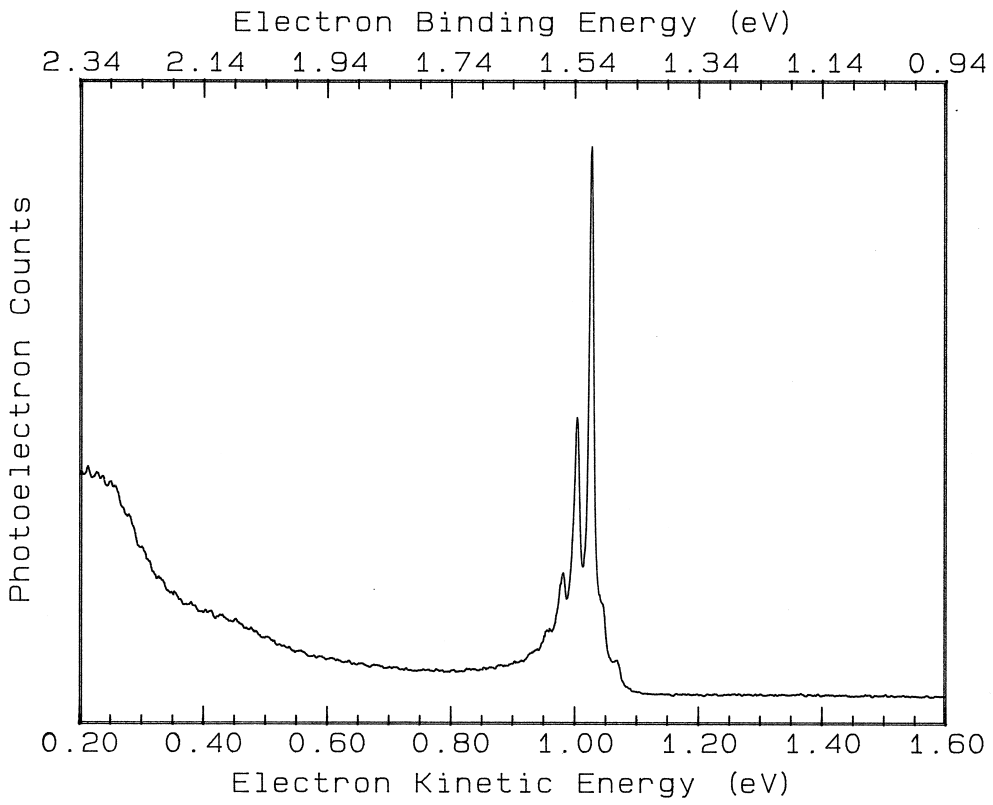

Fig. 2. 488.0 nm (2.540 eV) photoelectron spectrum of Nb_8^- prepared in the fully liquid nitrogen cooled flow tube.

[69]). Spectra obtained with the mass analyzer adjusted to more than halfway down the left or right slopes of the Nb_8^- mass peak did not differ significantly, demonstrating the lack of contributions from possible unresolved impurities such as hydrides. These are likely contaminants in niobium cluster studies, and we did occasionally observe Nb_3H^- and $Nb_3H_2^-$ under similar source conditions [68].

In the 488 nm (2.540 eV) spectrum, the origin peak appears at an eKE of 1.027 ± 0.004 eV (peak center) with a full width at half maximum intensity (FWHM) of 9 meV, as given by Gaussian fits. The former value corresponds to an adiabatic electron affinity of 1.513 ± 0.008 eV for Nb_8, assuming that the observed states of Nb_8^- and Nb_8 are indeed their ground electronic states. The larger experimental uncertainty of 8 meV quoted for this value exceeds the 4 meV uncertainty estimated for the O^- calibration to take into account possible shifts of the true $v_{neutral} = 0 \leftarrow v_{anion} = 0$ transition from the observed peak center due to unresolved vibrational sequence bands, as is further discussed below. The electron affinity measured here is consistent with the result of ~1.5 eV obtained in the UV photoelectron study [52,53].

The weak shoulder on the right of the origin band is assigned as the $v_{neutral} = 0 \leftarrow v_{anion} = 1$ hot band. As shown in the inset to the figure, the relative intensity of this feature is enhanced in the spectrum of warmer anions prepared by removing the liquid nitrogen coolant from the 18 in. long section of the flow tube nearest the nosecone. The positions of the shoulders in both spectra indicate a frequency of 165 ± 20 cm^{-1} for the active mode in the anion. The "cold" spectrum also exhibits a weak peak about 330 cm^{-1} to the right of the origin. While the position of this feature is consistent with its assignment as the $0 \leftarrow 2$ hot band, its intensity is greater than expected, as discussed in the next section.

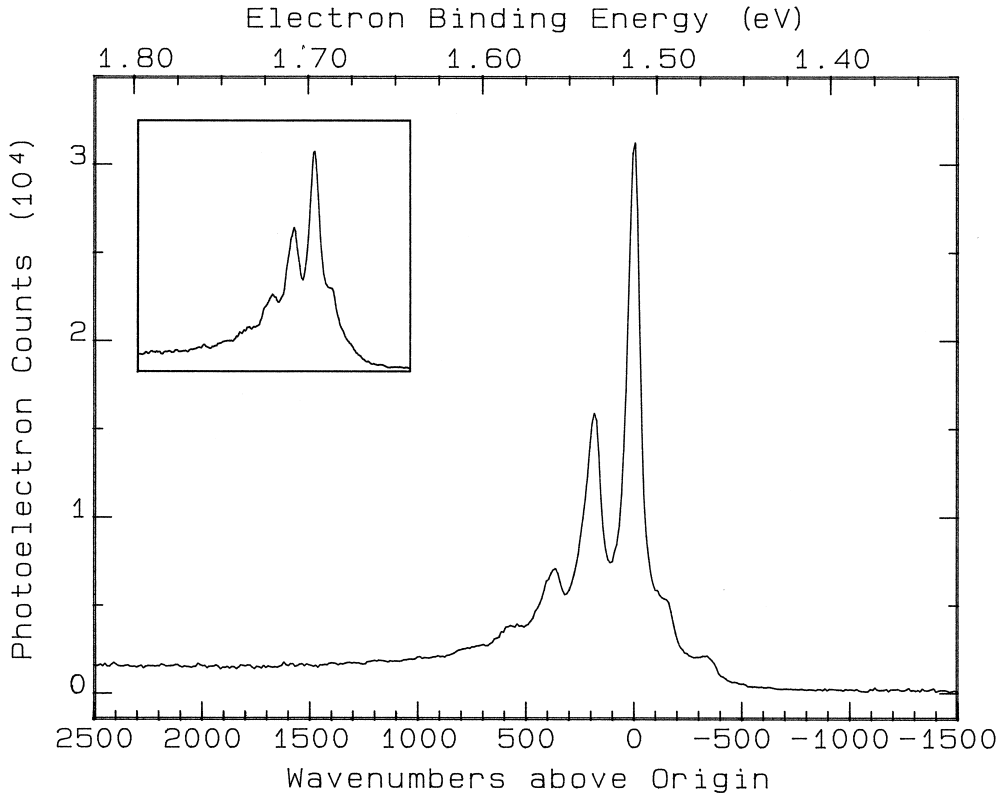

Fig. 3. Expansion of the vibrationally resolved region of Fig. 2. The inset shows the spectrum of warmer Nb_8^- anions prepared without liquid nitrogen cooling of the downstream section of the flow tube.

A large reduction of ~30% in the anion beam current, as measured by a large Faraday cup terminating the anion beam line 3 in. past the laser beam crossing, was noted when the laser was operating at its usual intracavity power of ~100 W. Since undoubtedly some of the anions reaching the Faraday cup did not traverse the tightly focussed laser beam, these results suggest that a very large fraction of the anions that did so were photodetached (or photodissociated with fragment anions scattering out of the detected region). As expected for a direct photodetachment process, scans of the origin band region obtained with the laser power reduced sufficiently to decrease the detected anion current by only 10% displayed the same peak widths (and height relative to the $1 \leftarrow 0$ peak) as were observed at the higher laser power.

The ≥9 meV peak widths observed in Fig. 3 substantially exceed the ~5 meV instrumental resolution. It is likely that this additional broadening is due mainly to unresolved vibrational sequence bands; broadening due to rotational structure is expected to be relatively insignificant. Fournier et al. [51] have predicted the 18 vibrational modes of Nb_8^- to have frequencies of 107–320 cm^{-1}. Sequence ($\Delta v = 0$) transitions can occur from excited levels of all of these modes. Even at the low temperature of 150 K estimated from the Franck-Condon simulation described in the following section, this high density of states gives a harmonic vibrational partition function of 20, implying that only 5% of the Nb_8^- anions populate the zero point vibrational level. If vibrational frequencies differ in the neutral and anionic clusters, sequence transitions from excited vibrational levels will be displaced from the corresponding zero point transitions, producing thermal broadening. Many of

the vibrational modes are indeed predicted [51] to have higher frequencies in neutral Nb_8 than in Nb_8^-. This direction of change would generate sequence bands on the left of the $n \leftarrow 0$ transitions, also shifting the observed origin band to a higher binding energy than the true adiabatic electron affinity (hence the increased error bar quoted above for this value). The spectrum of the warmer anions shown in the inset to Fig. 3 exhibits broader peaks, as expected. At the temperature of 270 K estimated from this spectrum, the vibrational partition function increases to 1800, corresponding to only 0.05% of the Nb_8^- anions in the zero point level.

The higher electron binding energy (eBE) region of the spectrum shown in Fig. 2 displays an elevated baseline to the left of the structured 1.5 eV (eBE) transition, then a gradually increasing intensity starting at ~1.9 eV, with a levelling off near 2.3 eV. The sensitivity of our instrument degrades rapidly at higher binding energies (≤0.2 eV eKE). The full spectrum of the anions prepared in the warmer flow tube (not shown) displays the same features with the same relative intensities, consistent with their assignment to the same anion state that gives rise to the structured transition. These features are also observed in the UV spectra reported by Kietzmann et al., but our spectrum does not show the valley near 2.15 eV that appears in the 3.49 eV spectrum [52]. In addition, the high eBE region of our spectrum appears much less intense, relative to the 1.5 eV region, than in the UV spectra [52,53]. For example, in our spectra obtained at both anion temperatures, the integrated intensity of the broad feature in the 2.15–2.35 eV region is 1.6 times greater than that of the structured transition (1.45–1.65 eV). In contrast, the ratio observed in the 3.49 eV spectrum [52] appears to be ~7. The $(eKE)^{1/2}$ dependence of photodetachment cross sections [11] accounts for a reduction of about a factor of 1.5 in this ratio in our 2.540 eV spectrum, and our instrumental sensitivity is typically reduced by ~30% at 2.34 eV (0.20 eV eKE). These considerations reduce the apparent discrepancy between the relative intensities in the two spectra to about a factor of 2. Resonances of the laser with metastable anion states can also affect observed intensity ratios. An additional factor that may contribute to a greater relative intensity of the high eBE peak in the UV spectrum may be a greater extent of *d* character in the orbitals from which the electrons are detached in the transitions in that region, versus a greater extent of *s* or *sp* character for the 1.5 eV transition [12,70]. In 2.540 eV photoelectron spectra of the first and second series transition metal atoms, the cross sections for *d* electron detachments are much lower than those for *s* electron detachments [71].

4. Data analysis

4.1. Franck-Condon fit

Fig. 4 shows one-dimensional harmonic Franck-Condon fits (sticks and dashed lines) to the observed spectra (solid lines), with labels ($v_{neutral} \leftarrow v_{anion}$) indicating the main contribution to each peak. The fits were generated using the program PESCAL [72], for frequencies of 180 cm^{-1} for Nb_8 and 165 cm^{-1} for Nb_8^-, and a normal mode displacement of 0.41 $amu^{1/2}$ Å. The fit to the spectrum of the colder ions assumes a vibrational temperature of 150 K, while that for the warmer ions, shown in the inset, assumes 270 K. These temperatures were determined from the relative intensities of the origin and the $0 \leftarrow 1$ hot bands. The simulations of the 150 and 270 K spectra employed Lorentzian lineshapes with widths (FWHM) of 10 and 15 meV, respectively. The displacement is reported with a generous error bar as 0.4 ± 0.1 $amu^{1/2}$ Å to encompass results obtained with different fitting parameters. (This value refers to the magnitude of the normal mode displacement; a harmonic Franck-Condon analysis cannot determine its sign.)

The good agreement between the observed and simulated spectra supports the assignment of these peaks as a vibrational progression in a single electronic transition. Even the increased broadening of the peaks labelled $1 \leftarrow 0$, $2 \leftarrow 0$, and $3 \leftarrow 0$ is partially reproduced by the increased intensities calculated for the sequence transitions ($v_{neutral} = m + n \leftarrow v_{anion} = m$) in the active mode that appear to the left (because $v_{neutral} > v_{anion}$) of the $n \leftarrow 0$ transi-

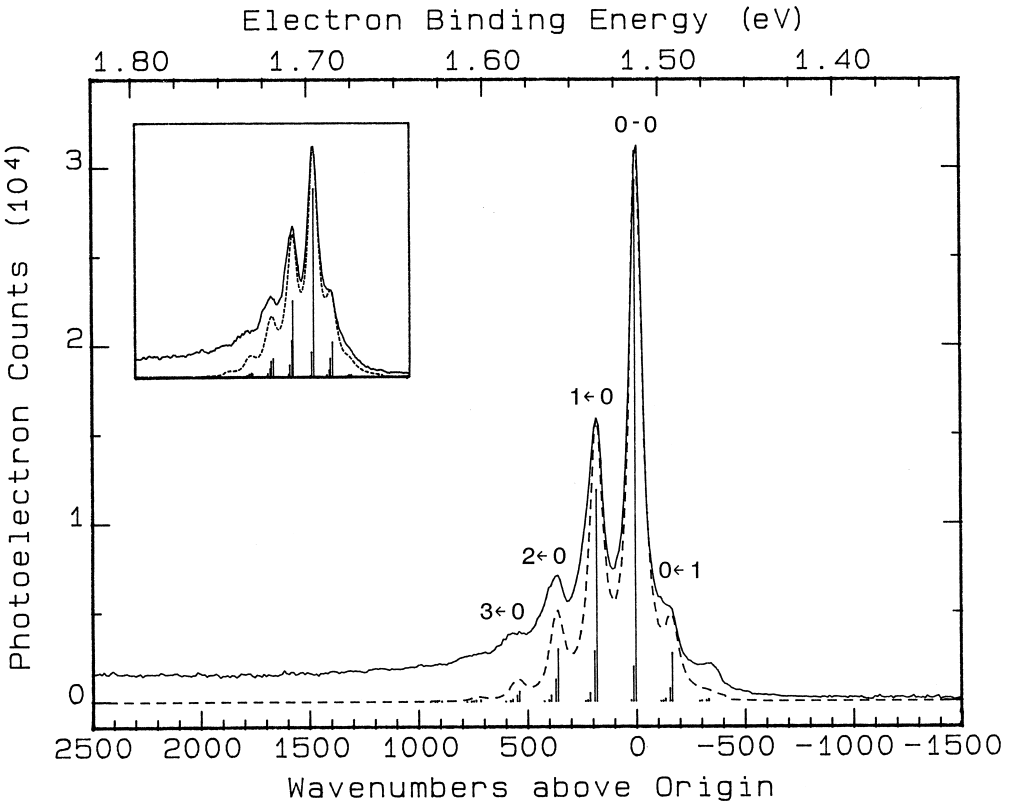

Fig. 4. One-dimensional harmonic Franck-Condon fits (dashed lines and sticks) of the spectra in Fig. 3, showing a progression in a mode with a frequency of 180 cm^{-1} in Nb_8 and 165 cm^{-1} in Nb_8^- and a normal mode displacement of 0.41 $amu^{1/2}$ Å. Temperatures and linewidths (FWHM, Lorentzian) of 150 K, 10 meV (main spectrum) and 270 K, 15 meV (inset) were used. Assignments ($v_{neutral} \leftarrow v_{anion}$) indicate the main contribution to each peak.

tions. However, the intensity of the weak peak assigned as the $0 \leftarrow 2$ hot band is underestimated in the "cold" simulated spectrum; its intensity relative to the origin is better fit by a temperature of ~400 K. This (unresolved) region of the 270 K spectrum appears with about the expected intensity. The anomalous intensity of this feature in the former spectrum may reflect less complete vibrational equilibration of the anions prepared in the colder flow tube, as we have also observed in the spectrum of VMn^- [68]. Or, this weak feature may only coincidentally appear at the position expected for the $0 \leftarrow 2$ hot band, and may actually arise from an excited electronic state or isomer of Nb_8^-.

While satisfactory, this fit to the spectrum is certainly not unique. For example, there may be additional active modes with smaller displacements producing weaker features hidden beneath the main peaks, or the apparent single progression may actually consist of overlapping, individually unresolved progressions.

4.2. Approximate normal mode analyses

In view of the small displacement of 0.4 ± 0.1 $amu^{1/2}$ Å measured for the observed mode, and the absence of more extensive vibrational activity, it is likely that the observed states of Nb_8^- and Nb_8 have the same symmetry, and therefore that the active mode is totally symmetric. With this assumption, two different approaches employing FG matrix methods [73] were used to attempt to translate this normal

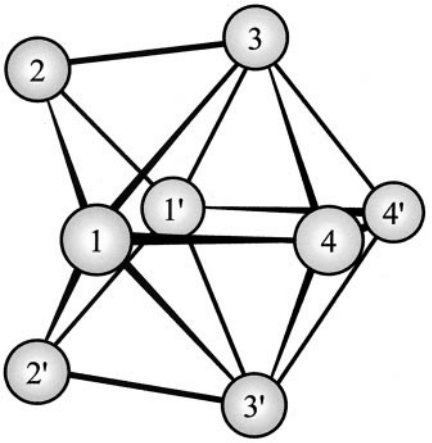

Fig. 5. Calculated C_{2v} ground state structure of Nb_8 and Nb_8^- [50–52], a bicapped distorted octahedron with four inequivalent atoms. Equilibrium lengths (Å) for the 17 bonds (<3 Å) reported in Ref. 51 for Nb_8^- are 2.44 (2–3 × 2 bonds), 2.46 (1–4 × 2), 2.47 (1–2 × 4), 2.56 (3–4 × 4), 2.57 (4–4′), and 2.83 (1–3 × 4), giving an average bond length of 2.58 Å. By comparison, the $^3\Sigma_g^-$ ground state of Nb_2 has a short bond length of 2.0778 Å [75], and the nearest neighbor distance in bulk niobium is 2.86 Å [86]. Nb atomic radial expectation values are 1.134 Å for the 4*d* and 2.144 Å for the 5*s* orbitals [87].

mode displacement into bond length differences between Nb_8^- and Nb_8.

We first assumed the highest possible (nonplanar) geometric symmetry, a cubic O_h structure which will have only one totally symmetric vibrational mode, the breathing mode. In this case, the magnitude of the L matrix element that converts the measured normal mode displacement (ΔQ) into a displacement in terms of this A_{1g} symmetry coordinate (ΔS = L ΔQ) is simply $(2/m)^{1/2} = 0.147$ (the square root of the corresponding G matrix element), where m = 92.9 amu for Nb. The measured ΔQ value of 0.4 amu$^{1/2}$ Å then corresponds to a value of 0.06 Å for ΔS. The change in an individual Nb–Nb bond length, Δr, is then $\Delta S/\sqrt{12}$, or 0.02 Å.

In a second approach, we assumed the C_{2v} bicapped octahedral geometry shown in Fig. 5, which is calculated [50–52] to be the lowest energy structure for Nb_8^- and Nb_8. Since this cluster has seven totally symmetric (A_1) vibrational modes, the corresponding L matrix elements now also depend on the equilibrium bond lengths and vibrational force constants. We assumed the 17 bond lengths (<3 Å) reported by Fournier et al. [51], and set $r(1–1') = r(2–2') =$ 3.15 Å. To estimate the force constants, we used the "bond-connectivity" force field proposed by Ozin and McIntosh [74]. In this model, the internal coordinates of a metal cluster are defined as bond stretches involving nearest-neighbor atoms. The primary stretching force constant (f_r) associated with each bond is then estimated to be $(2/a)$ times f_r for the metal dimer, where a is the total number of bonds to the 2 bonded atoms in the cluster and the numerator gives $a = 2$ for the dimer. The 4.95 mdyn/Å Nb_2 force constant [75] then gives f_r values ranging from 0.99 to 1.24 mdyn/Å for the 17 Nb_8 bonds. The 1–1′ and 2–2′ stretches were also defined as internal coordinates (giving one redundant coordinate), with f_r varied from 0.59 mdyn/Å (half the 1.17 mdyn/Å value in Ag_2) [76] to 0.30 mdyn/Å. Interaction force constants (f_{rr}) were varied from 0 as initially assumed to 5% or to 10% of the average f_r value for bond pairs sharing a common atom (in view of arguments in the literature that metal clusters will have positive interaction constants [77] as is also the case for Nb_3 [17]), or to the values recommended by Ozin and McIntosh [74] based upon results [78] for $[B_{12}H_{12}]^{2-}$. Calculations were also done referencing the f_r values to Nb_3 [17], giving $f_r = (4/a)1.95$ mdyn/Å, or assuming the equilibrium bond lengths obtained in the BLYP calculations [50,79] by Grönbeck et al.

With these seven sets of assumed bond lengths and force constants, we used the vibrational analysis programs written by McIntosh and Peterson [80] to calculate the vibrational frequencies, the L matrix, and other vibrational properties. Although the overall frequency range naturally varied with the different force constants assumed, the nature of the A_1 modes in the 150–200 cm^{-1} range, which provide the most likely assignments for the active mode in the spectrum (180 ± 15 cm^{-1} Nb_8, 165 ± 20 cm^{-1} Nb_8^-), were relatively invariant. The symmetric breathing mode consistently appeared as the highest frequency mode (at 249–357 cm^{-1}), whereas those in the 150–200 cm^{-1} range involved the contraction of some bonds while others expanded. Thus, assigning the active mode as one of these implies that some bonds in Nb_8^-

contract and others expand on electron detachment. For each of the seven sets of assumed parameters, and for the one or two A_1 modes found in each case to fall within the 150–200 cm^{-1} range, the corresponding symmetrized L matrix elements indicated that the observed 0.4 $amu^{1/2}$ Å normal mode displacement corresponds to an average value of 0.005–0.008 Å for the magnitudes of the 17 bond length differences between Nb_8^- and Nb_8. A narrow range of 0.015–0.022 Å was also obtained for the largest individual bond length change (which appeared along equatorial bonds).

These results are in surprisingly good agreement with the Nb_8^- and Nb_8 bond lengths calculated by Grönbeck et al. [50,79]. Their BLYP results also show some of the bonds in Nb_8^- to contract and others to expand on electron detachment, with an average value of 0.007 Å for the magnitudes of the bond length differences, and a largest change of 0.024 Å (a contraction of the 4–4′ equatorial bond).

5. Discussion

The photoelectron spectrum of Nb_8^-, obtained at 488 nm (2.540 eV) and with an instrumental resolution of ~5 meV, displays a vibrational progression in a mode whose frequency is 180 ± 15 cm^{-1} in the neutral cluster and 165 ± 20 cm^{-1} in the anion. Thus, according to the Franck-Condon principle, the displacement in equilibrium geometries between these states of Nb_8^- and Nb_8 occurs mainly along this normal coordinate. The lack of more extensive vibrational activity suggests that these states have the same symmetry and therefore that the active mode is totally symmetric. The small normal mode displacement of 0.4 ± 0.1 $amu^{1/2}$ Å, obtained from the Franck-Condon analysis described in Sec. 4.1, indicates that the Nb–Nb bond lengths change very little upon electron detachment. The approximate FG matrix analyses described in Sec. 4.2 suggest bond length differences under 0.03 Å. The similarity between the spectrum reported here and the previously reported UV spectra [52,53] indicates that the same state of Nb_8^- was observed in both experiments.

Before discussing the possible structures of Nb_8^- and Nb_8 observed in this experiment, we note that these are not necessarily their lowest energy structures. The geometry of the neutral cluster observed in the photoelectron spectrum cannot differ radically from that of the anion in view of Franck-Condon overlap requirements. In addition, it is possible that the Nb_8^- structure prepared in our flowing afterglow reactor, where larger clusters can grow from smaller ones by ion-neutral reactions, may be kinetically rather than thermodynamically controlled. Niobium-carbon clusters provide a dramatic example of this phenomenon, as they exhibit different growth patterns under various experimental conditions in gas phase plasma reactions, yielding either metallo-carbohedrene ("met-car") cage structures or cubic structures [81].

The surprisingly simple vibrational structure in the photoelectron spectrum is most easily understood if the observed Nb_8^- and Nb_8 clusters have highly symmetric structures, and therefore relatively few totally symmetric vibrational modes. For example, if both clusters were to have cubic geometries, only progressions in the single totally symmetric (breathing) mode would be allowed. The analogous argument was employed by Smalley and co-workers to deduce a planar D_{6h} structure for Au_6^-, whose higher resolution autodetachment spectrum also displays a single vibrational progression [34]. There are, indeed, a rapidly growing number of ligated transition metal cluster complexes known to incorporate a cubic M_8 core [82,83]. An early example was $Ni_8(CO)_8(\mu_4\text{-}PC_6H_5)_6$, whose short Ni–Ni distances of ~2.6 Å are indicative of Ni–Ni bonding [84]. About 20 analogous compounds have now been structurally characterized [82]. The bare Cr_8 cluster has been predicted by DFT calculations to have a flattened cubic structure [12,85]. Bulk niobium has a body-centered cubic structure [86].

However, the LSDA DFT study of Nb_8^- by Fournier et al. did investigate a cubic structure, as well as other highly symmetric structures such as the D_{4d} square antiprism and the T_d tetracapped tetrahedron [51]. These trial structures were found not to lead to plausible isomers, as they had a very high

energy, possessed imaginary frequencies (were not local minima), or relaxed to a lower symmetry upon optimization [51]. Grönbeck et al. found the T_d tetracapped tetrahedron to be a high energy ($\geq$1.5 eV) local minimum for Nb_8 [50]. As noted above, it is possible that the isomer of Nb_8^- and Nb_8 observed here differs from the thermodynamically most stable structures, and may conceivably be one of the highly symmetric isomers predicted at relatively high energy.

In contrast, the ground states of Nb_8^- and Nb_8 are predicted to have only C_{2v} symmetry [50–52]. The electron detachment energy calculated for this structure in the LSDA (1.55 eV) [51] and BLYP (1.19 eV) [50] studies, as well as its predicted higher electron binding energies [52], are in reasonable agreement with the photoelectron spectra, and Kietzmann et al. concluded that their 3.49 eV spectrum is due almost purely to this isomer [52]. This C_{2v} structure, shown in Fig. 5, would have seven totally symmetric (A_1) vibrational modes. Although it may seem unlikely that this fairly low symmetry structure would give rise to the simple vibrational structure observed here, it is possible. As noted in Sec. 4.1, the $\geq$9 meV ($\geq$70 cm^{-1}) widths in our spectrum result in overlapping peaks in the 180 cm^{-1} progression, which may obscure the weaker activities of additional vibrational modes. In addition, not only symmetry considerations but also Franck-Condon factors constrain the number of vibrational modes active in a photoelectron spectrum. Indeed, the approximate FG matrix analysis described in Sec. 4.2 gave excellent agreement with the average (0.007 Å) and largest (0.024 Å) magnitudes of the equilibrium bond length differences between Nb_8^- and Nb_8 calculated by Grönbeck et al. [50,79] for this structure. However, our approximate vibrational analysis is not capable of deducing more specific bond length differences for comparison with the theoretical results. It is possible that the predicted changes in the Nb_8^- and Nb_8 bond lengths would correspond to displacements along several normal coordinates, leading to a more congested spectrum than is actually observed.

Another possibility for the observed isomer is a higher symmetry D_{3d} structure. A quartet D_{3d} bicapped triangular antiprismatic state of Nb_8^- was calculated by Fournier et al. at 1.21 eV, with an electron binding energy of 1.71 eV, similar to the 1.55 eV value obtained for the C_{2v} isomer [51,52]. However, the higher electron binding energies calculated for this state were considered to give a relatively poor match to the UV photoelectron spectrum [52]. A doublet D_{3d} state with a significantly different structure was calculated in the BLYP studies by Grönbeck et al. to lie only 0.24 eV above the Nb_8^- ground state [50]. The electron detachment energy of Nb_8^- (1.16 eV) and the HOMO-LUMO gap of Nb_8 (0.96 eV) calculated for this isomer were close to those obtained for the C_{2v} ground state (1.19, 0.79 eV respectively) [50].

On the other hand, two low energy isomers of Nb_8^- and Nb_8 identified in the DFT studies can be excluded as likely candidates for the observed structure. A C_1 isomer was calculated to lie 1.05 eV above the C_{2v} ground state of Nb_8^- in the LSDA [51,52] and 0.76 eV in the BLYP [50] studies. The electron detachment energy obtained in the LSDA (1.63 eV) [51] and BLYP (1.29 eV) [50] calculations is in each case close to that of the C_{2v} structure (1.55 and 1.19 eV, respectively). The higher electron binding energies predicted for the two isomers are also similar [52], as are the calculated HOMO-LUMO gaps in neutral Nb_8 (0.79 eV C_{2v}, 0.63 eV C_1) [50]. Accordingly, Kietzmann *et al*. assigned their 4.0 eV photoelectron spectrum to a combination of the C_{2v} and C_1 isomers [52]. However, the single vibrational progression observed in the present study does not appear compatible with a C_1 structure, as all 18 vibrational modes of this asymmetrical cluster would be allowed to be active in the spectrum.

A higher symmetry D_{2d} (trigonal dodecahedral) structure was identified by Grönbeck et al. as another low energy isomer, lying only 0.30 eV above the C_{2v} ground state of Nb_8^- in their BLYP calculations [50]. (This structure was not concluded by Fournier et al. to be a plausible isomer, although it was considered [51].) A D_{2d} Nb_8 cluster would have only four totally symmetric vibrational modes, and four symmetrically inequivalent bonds (as it is related to the C_{2v} structure shown in Fig. 5, but has equal lengths for bond pairs

2–2′ and 4–4′, 1–4 and 2–3, 1–2 and 3–4). In addition, the electron affinity of 1.55 eV obtained for the D_{2d} isomer of Nb_8 in the BLYP calculations, which was 0.3–0.4 eV higher than those of the other four isomers studied, is in excellent agreement with the measured value of 1.513(8) eV. Other bare metal octamers, including Ag_8^- and Ag_8 [88], have been predicted to have D_{2d} ground states. Riley and coworkers concluded that the bare Ni_8 cluster has a D_{2d} dodecahedral structure based upon results of N_2 and NH_3 uptake experiments [89]. However, in contrast to the other four structures studied, the D_{2d} isomer of Nb_8 is calculated by Grönbeck et al. to have a bonding LUMO [50]. Addition of an extra electron to this orbital to form the anion would be expected to produce a substantial geometry change, as is indicated by the large difference of 0.23 eV between the vertical electron affinity (1.44 eV) and detachment energy (1.67 eV) calculated for this structure [50]. This result is not compatible with the short vibrational progression observed in the photoelectron spectrum.

A unique identification of the isomer of Nb_8 and Nb_8^- observed in these experiments could potentially be obtained from a comparison of the vibrationally resolved transition to spectra predicted based on Franck-Condon analyses of the calculated geometries and vibrational descriptions for different possible structures. This approach has very successfully been used to identify the structures of the Nb_3O [26], Nb_3N_2 [27], and Nb_3C_2 [28] neutral and cationic clusters observed in higher resolution, zero electron kinetic energy photoelectron spectra. It is hoped that the results reported here will stimulate such calculations for the even more computationally challenging Nb_8 and Nb_8^- clusters, and perhaps thereby also serve as a useful benchmark for theoretical studies of other clusters of open *d*-shell transition metals.

Acknowledgements

We thank Dr. H. Grönbeck, Dr. W. Andreoni, and Dr. A. Rosén for sending us their ground state structures, and Dr. Evan Millam and Ms. Nancy Fleischer for their assistance with these experiments. We are grateful for Prof. Bob Squires' insights on niobium cluster ion-molecule chemistry during his visit to our Department last May. Acknowledgement is made to the Donors of The Petroleum Research Fund, administered by the American Chemical Society, for support of this research.

References

[1] M.A. Duncan (Ed.), Advances in Metal and Semiconductor Clusters, Vols. 1–4, JAI, Greenwich, 1993–1998.
[2] N. Russo, D.R. Salahub (Eds.), Metal-Ligand Interactions: Structure and Reactivity, NATO ASI Series C, Mathematical and Physical Sciences, Vol. 474, Kluwer Academic, Dordrecht, 1996.
[3] A.W. Castleman Jr., K.H. Bowen Jr., J. Phys. Chem. 100 (1996) 12 911.
[4] P.E.M. Siegbahn, Adv. Chem. Phys. 93 (1996) 333; B.O. Roos, K. Andersson, M.P. Fülscher, P.-Å. Malmqvist, L. Serrano-Andrés, Adv. Chem. Phys. 93 (1996) 219.
[5] R. Fournier, I. Pápai, in D.P. Chong (Ed.), Recent Advances in Density Functional Methods, Part I, World Scientific, Singapore, 1995, pp. 219–285.
[6] U. Kreibig, M. Vollmer, Optical Properties of Metal Clusters, Springer Series in Materials Science, Vol. 25, Springer-Verlag, Berlin, 1995.
[7] H. Haberland (Ed.), Clusters of Atoms and Molecules, Springer Series in Chemical Physics, Vols. 52 and 56, Springer-Verlag, Berlin, 1994.
[8] D.C. Parent, S.L. Anderson, Chem. Rev. 92 (1992) 1541.
[9] L. Andrews, M. Moskovits (Eds.), Chemistry and Physics of Matrix-Isolated Species, Elsevier, Amsterdam, 1989.
[10] M.D. Morse, Chem. Rev. 86 (1986) 1049–1109.
[11] K.M. Ervin, W.C. Lineberger, in N.G. Adams, L.M. Babcock (Eds.), Advances in Gas Phase Ion Chemistry, Vol. I, JAI, Greenwich, 1992, pp. 121–166.
[12] L.-S. Wang, H. Wu, in M.A. Duncan (Ed.), Advances in Metal and Semiconductor Clusters, Vol. 4, JAI, Greenwich, 1998, pp. 299–343; L.-S. Wang, H. Wu, Z. Physik. Chem. 203 (1998) 45.
[13] P.A. Hackett, S.A. Mitchell, D.M. Rayner, B. Simard, in N. Russo, D.R. Salahub (Eds.), Metal-Ligand Interactions: Structure and Reactivity, NATO ASI Series C, Mathematical and Physical Sciences, Vol. 474, Kluwer Academic, Dordrecht, 1996, pp. 289–324.
[14] M. Moskovits, D.P. DiLella, W. Limm, J. Chem. Phys. 80 (1984) 626.
[15] H. Haouari, H. Wang, R. Craig, J.R. Lombardi, D.M. Lindsay, J. Chem. Phys. 103 (1995) 9527; H. Wang, Z. Hu, H. Haouari, R. Craig, Y. Liu, J.R. Lombardi, D.M. Lindsay, J. Chem. Phys. 106 (1997) 8339.
[16] D.-S. Yang, A.M. James, D.M. Rayner, P.A. Hackett, Chem. Phys. Lett. 231 (1994) 177.

[17] H. Wang, R. Craig, H. Haouari, Y. Liu, J.R. Lombardi, D.M. Lindsay, J. Chem. Phys. 105 (1996) 5355.
[18] D.P. DiLella, W. Limm, R.H. Lipson, M. Moskovits, K.V. Taylor, J. Chem. Phys. 77 (1982) 5263; G.A. Ozin, S.A. Mitchell, Angew. Chem. Int. Ed. Engl. 22 (1983) 674; G.A. Ozin, M.D. Baker, S.A. Mitchell, D.F. McIntosh, Angew. Chem. Int. Ed. Engl. 22 (1983) 166; J. Derouault, M. Dalibart, Z. Phys. D—Atoms, Molecules and Clusters 19 (1991) 211.
[19] K.D. Bier, T.L. Haslett, A.D. Kirkwood, M. Moskovits, J. Chem. Phys. 89 (1988) 6.
[20] J.R. Woodward, S.H. Cobb, J.L. Gole, J. Phys. Chem. 92 (1988) 1404; M. Moskovits, D.P. DiLella, J. Chem. Phys. 72 (1980) 2267.
[21] K.M. Ervin, J. Ho, W.C. Lineberger, J. Chem. Phys. 89 (1988) 4514.
[22] A. O'Keefe, J.J. Scherer, A.L. Cooksy, R. Sheeks, J. Heath, R.J. Saykally, Chem. Phys. Lett. 172 (1990) 214; M.D. Morse, Chem. Phys. Lett. 133 (1987) 8; W.H. Crumley, J.S. Heyden, J.L. Gole, J. Chem. Phys. 84 (1986) 5250; E.A. Rohlfing, J.J. Valentini, Chem. Phys. Lett. 126 (1986) 113; M. Moskovits, Chem. Phys. Lett. 118 (1985) 111; D.P. DiLella, K.V. Taylor, M. Moskovits, J. Phys. Chem. 87 (1983) 524; M.D. Morse, J.B. Hopkins, P.R.R. Langridge-Smith, R.E. Smalley, J. Chem. Phys. 79 (1983) 5316.
[23] T. Okazaki, Y. Saito, A. Kasuya, Y. Nishina, J. Chem. Phys. 104 (1996) 812; P.Y. Cheng, M.A. Duncan, Chem. Phys. Lett. 152 (1988) 341; U. Kettler, P.S. Bechtold, W. Krasser, Surf. Sci. 156 (1985) 867; W. Schulze, H.U. Becker, R. Minkwitz, K. Manzel, Chem. Phys. Lett. 55 (1978) 59.
[24] G.A. Bishea, M.D. Morse, J. Chem. Phys. 95 (1991) 8779.
[25] J.C. Pinegar, J.D. Langenberg, M.D. Morse, Chem. Phys. Lett. 212 (1993) 458; G.A. Bishea, C.A. Arrington, J.M. Behm, M.D. Morse, J. Chem. Phys. 95 (1991) 8765.
[26] D.-S. Yang, M.Z. Zgierski, D.M. Rayner, P.A. Hackett, A. Martinez, D.R. Salahub, P.-N. Roy, T. Carrington Jr., J. Chem. Phys. 103 (1995) 5335.
[27] D.-S. Yang, M.Z. Zgierski, A. Bérces, P.A. Hackett, A. Martinez, D.R. Salahub, Chem. Phys. Lett. 227 (1997) 71.
[28] D.-S. Yang, M.Z. Zgierski, A. Bérces, P.A. Hackett, P.-N. Roy, A. Martinez, T. Carrington Jr., D.R. Salahub, R. Fournier, T. Pang, C. Chen, J. Chem. Phys. 105 (1996) 10663.
[29] D.-S. Yang, M.Z. Zgierski, P.A. Hackett, J. Chem. Phys. 108 (1998) 3591.
[30] H. Wang, R. Craig, H. Haouari, J.-G. Dong, Z. Hu, A. Vivoni, J.R. Lombardi, D.M. Lindsay, J. Chem. Phys. 103 (1995) 3289.
[31] M.F. Jarrold, K.M. Creegan, Chem. Phys. Lett. 166 (1990) 116.
[32] T.L. Haslett, K.A. Bosnick, M. Moskovits, J. Chem. Phys. 108 (1998) 3453.
[33] H. Handschuh, G. Ganteför, W. Eberhardt, Rev. Sci. Instrum. 66 (1995) 3838.
[34] K.J. Taylor, C. Jin, J. Conceicao, L.-S. Wang, O. Cheshnovsky, B.R. Johnson, P.J. Nordlander, R.E. Smalley, J. Chem. Phys. 93 (1990) 7515; G.F. Gantefor, D.M. Cox, A. Kaldor, J. Chem. Phys. 96 (1992) 4102.
[35] M.L. Cohen, M.Y. Chou, W.D. Knight, W.A. de Heer, J. Phys. Chem. 91 (1987) 3141.
[36] C.E. Moore, Atomic Energy Levels, Natl. Bur. Stand. Circ. 467, U.S. GPO, Washington, D.C., 1952, 1958.
[37] M.E. Geusic, M.D. Morse, R.E. Smalley, J. Chem. Phys. 82 (1985) 590.
[38] M.D. Morse, M.E. Geusic, J.R. Heath, R.E. Smalley, J. Chem. Phys. 83 (1985) 2293.
[39] Y.M. Hamrick, M.D. Morse, J. Phys. Chem. 93 (1989) 6494.
[40] A. Bérces, P.A. Hackett, L. Lian, S.A. Mitchell, D.M. Rayner, J. Chem. Phys. 108 (1998) 5476.
[41] P.J. Brucat, C.L. Pettiette, S. Yang, L.-S. Zheng, M.J. Craycraft, R.E. Smalley, J. Chem. Phys. 85 (1986) 4747.
[42] M.R. Zakin, R.O. Brickman, D.M. Cox, A. Kaldor, J. Chem. Phys. 88 (1988) 3555.
[43] J.L. Elkind, F.D. Weiss, J.M. Alford, R.T. Laaksonen, R.E. Smalley, J. Chem. Phys. 88 (1988) 5215.
[44] R.L. Whetten, M.R. Zakin, D.M. Cox, D.J. Trevor, A. Kaldor, J. Chem. Phys. 85 (1986) 1697.
[45] M.B. Knickelbein, S. Yang, J. Chem. Phys. 93 (1990) 5760.
[46] K. Athanassenas, D. Kreisle, B.A. Collings, D.M. Rayner, P.A. Hackett, Chem. Phys. Lett. 213 (1993) 105.
[47] D. Britton, J.D. Dunitz, Acta Cryst. A29 (1973) 362.
[48] H. Grönbeck, A. Rosén, Phys. Rev. B 54 (1996) 1549.
[49] H. Grönbeck, A. Rosén, W. Andreoni, Z. Phys. D 40 (1997) 206.
[50] H. Grönbeck, A. Rosén, W. Andreoni, Phys. Rev. A 58 (1998) 4630.
[51] R. Fournier, T. Pang, C. Chen, Phys. Rev. A 57 (1998) 3683.
[52] H. Kietzmann, J. Morenzin, P.S. Bechthold, G. Ganteför, W. Eberhardt, D.-S. Yang, P.A. Hackett, R. Fournier, T. Pang, C. Chen, Phys. Rev. Lett. 77 (1996) 4528.
[53] H. Kietzmann, J. Morenzin, P.S. Bechthold, G. Ganteför, W. Eberhardt, J. Chem. Phys. 109 (1998) 2275.
[54] J.G. Eaton, L.H. Kidder, H.W. Sarkas, K.M. McHugh, K.H. Bowen, NATO ASI Ser. C 374 (1992) 493.
[55] J. Ho, K.M. Ervin, W.C. Lineberger, J. Chem. Phys. 93 (1990) 6987; K.J. Taylor, C.L. Pettiette-Hall, O. Cheshnovsky, R.E. Smalley, J. Chem. Phys. 96 (1992) 3319; C.-Y. Cha, G. Ganteför, W. Eberhardt, J. Chem. Phys. 99 (1993) 6308; H. Handschuh, C.-Y. Cha, P.S. Bechthold, G. Ganteför, W. Eberhardt, J. Chem. Phys. 102 (1995) 6406.
[56] Y. Hamrick, S. Taylor, G.W. Lemire, Z.-W. Fu, J.-C. Shui, M.D. Morse, J. Chem. Phys. 88 (1988) 4095; M.B. Knickelbein, S. Yang, J. Chem. Phys. 93 (1990) 1476.
[57] S.K. Loh, L. Lian, P.B. Armentrout, J. Am. Chem. Soc. 111 (1989) 3167; D.A. Hales, L. Lian, P.B. Armentrout, Int. J. Mass Spectrom. Ion Processes 102 (1990) 269; 301; P.B. Armentrout in N. Russo, D.R. Salahub (Eds.), Metal-Ligand Interactions: Structure and Reactivity, NATO ASI Series C, Mathematical and Physical Sciences, Vol. 474, Kluwer Academic, Dordrecht, 1996, pp. 23–48.
[58] M.B. Knickelbein, W.J.C. Menezes, Phys. Rev. Lett. 69 (1992) 1046; W.J.C. Menezes, M.B. Knickelbein, J. Chem. Phys. 98 (1993) 1856.
[59] B.A. Collings, K. Athanassenas, D.M. Rayner, P.A. Hackett, Z. Phys. D 26 (1993) 36.
[60] A.A. Bengali, S.M. Casey, C.-L. Cheng, J.P. Dick, P.T. Fenn, P.W. Villalta, D.G. Leopold, J. Am. Chem. Soc. 114 (1992) 5257.

[61] S.T. Graul, R.R. Squires, Mass Spectrom. Rev. 7 (1988) 263.
[62] D.G. Leopold, J. Ho, W.C. Lineberger, J. Chem. Phys. 86 (1987) 1715.
[63] J. Cooper, R.N. Zare, J. Chem. Phys. 48 (1968) 942.
[64] H. Hotop, W.C. Lineberger, J. Phys. Chem. Ref. Data 14 (1985) 731.
[65] J. Mwakapumba, K.M. Ervin, Int. J. Mass Spectrom. Ion Processes 161 (1997) 161.
[66] E.L. Millam, Ph.D. Thesis, University of Minnesota, 1999.
[67] Q. Wu, S. Yang, Int. J. Mass Spectrom. 184 (1999) 57.
[68] T.P. Marcy, Ph.D. Thesis, University of Minnesota, 1999.
[69] S.M. Casey, D.G. Leopold, J. Phys. Chem. 97 (1993) 816.
[70] S. Hüfner, Photoelectron Spectroscopy, Springer-Verlag, Berlin, 1996, pp. 14–16.
[71] P.C. Engelking, W.C. Lineberger, Phys. Rev. A 19 (1979) 149; C.S. Feigerle, R.R. Corderman, S.V. Bobashev, W.C. Lineberger, J. Chem. Phys. 74 (1981) 1580.
[72] K.M. Ervin, W.C. Lineberger, unpublished FORTRAN program.
[73] E.B. Wilson Jr., J.C. Decius, P.C. Cross, Molecular Vibrations, Dover, New York, 1955.
[74] G.A. Ozin, D.F. McIntosh, J. Phys. Chem. 90 (1986) 5756.
[75] A.M. James, P. Kowalczyk, R. Fournier, B. Simard, J. Chem. Phys. 99 (1993) 8504.
[76] M.D. Morse, in M.A. Duncan (Ed.), Advances in Metal and Semiconductor Clusters, Vol. 1, JAI, Greenwich, 1993, p. 90.
[77] M. Moskovits, D.P. DiLella, in J.L. Gole, W.C. Stwalley (Eds.), Metal Bonding and Interactions in High Temperature Systems, ACS Symposium Series, Vol. 179, American Chemical Society, Washington, DC, 1982, pp. 169–172.
[78] L.L. Boyle, Y.M. Parker, Mol. Phys. 39 (1980) 95.
[79] H. Grönbeck, private communication.
[80] D.F. McIntosh, M.R. Peterson, "General Vibrational Analysis System," Quantum Chemistry Program Exchange, Program No. QCMP067.
[81] S. Wei, B.C. Guo, H.T. Deng, K. Kerns, J. Purnell, S.A. Buzza, A.W. Castleman Jr., J. Am. Chem. Soc. 116 (1994) 4475; C.S. Yeh, Y.G. Byun, S. Afzaal, S.Z. Kan, S. Lee, B.S. Freiser, P.J. Hay, J. Am. Chem. Soc. 117 (1995) 4042; J.S. Pilgrim, L.R. Brock, M.A. Duncan, J. Phys. Chem. 99 (1995) 544.
[82] J.-F. Halet, J.-Y. Saillard, Structure Bonding 87 (1997) 81.
[83] D.L. Kepert, in S.J. Lippard (Ed.), Progress in Inorganic Chemistry, Vol. 24, Wiley Interscience, New York, 1978, pp. 179–249.
[84] L.D. Lower, L.F. Dahl, J. Am. Chem. Soc. 98 (1976) 5046.
[85] H. Cheng, L.-S. Wang, Phys. Rev. Lett. 77 (1996) 51; L.-S. Wang, H. Wu, H. Cheng, Phys. Rev. B 55 (1997) 12884.
[86] C. Kittel, Introduction to Solid State Physics, Wiley, New York, 1976.
[87] J.P. Desclaux, Atomic Data and Nuclear Data Tables 12 (1973) 331.
[88] V. Bonacic-Koutecký, L. Češpiva, P. Fantucci, J. Pittner, J. Koutecký, J. Chem. Phys. 100 (1994) 490.
[89] E.K. Parks, L. Zhu, J. Ho, S.J. Riley, J. Chem. Phys. 100 (1994) 7206.